regions, the surface can be used for the local growth of a solution of functional molecules [29] or as a substrate for inkjet printing with functional molecules [30].

3.2. *Site-specific polymerization of methacrylate monomers*

The patterned organosilane monolayers are useful as template surfaces for site-specific polymerization by introducing organolsilane with an initiating unit. Atom transfer radical polymerization (ATRP) was employed with the patterned organosilane monolayer system. Since ATRP is one of the most successful methods for polymerizing a variety of monomers in a controlled fashion [31, 32] tailor-made surface topography is possible. Several reports have described the formation of polymer thin film by the radical polymerization from the immobilized ATRP initiator [33, 34].

Figure 10 shows a schematic representation of a site-specific atom transfer radical polymerization from a micropatterned monolayer surface. Prior to introducing the initiator for ATRP into the organosilane monolayer system, an AEAPDMS monolayer was prepared on a Si-wafer substrate surface. The prepared surface terminated by amino groups was treated with 2-bromoisobutyric acid in the presence of a condensation agent. After the modification, the water contact angle of the obtained surface increased from 63° to 69° due to the change of the surface functional groups. The introduction of the initiating unit was further confirmed by XPS measurement, in which the peaks attributed to Br and carbonyl carbon were observed at 68 eV and 287.9 eV, respectively. The resulting surface was

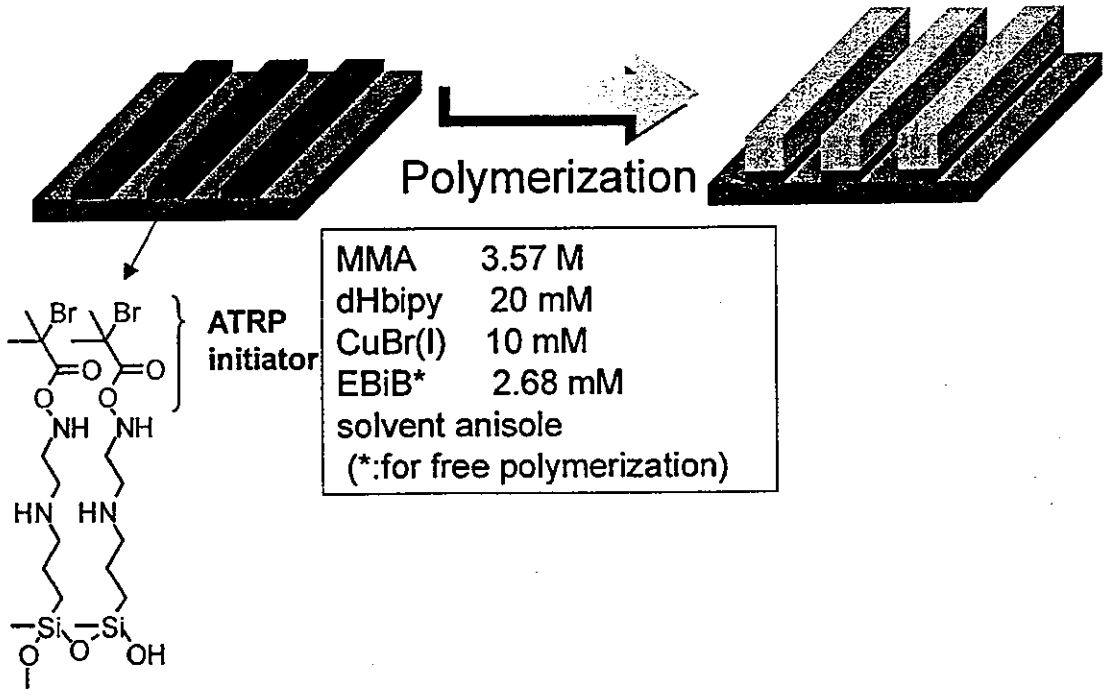

Figure 10. Schematic representation of the site-specific atom transfer radical polymerization from a micropatterned monolayer surface.

photoirradiated by VUV light through a photomask. The LFM image of the patterned surface shows the presence of a pattern corresponding to the line width of the photomask used. Furthermore, imaging ToF-SIMS revealed the complementary image of Br^- (m/z = 78.95) and SiO^- (m/z = 59.97) secondary ions. These results clearly revealed that the initiating groups for ATRP were area-selectively introduced on a Si wafer substrate surface.

Surface-initiated radical polymerization of methyl methacrylate (MMA) was carried out in the presence of CuBr(I) and 4,4′-di-*n*-heptyl-2,2′-bipyridine in anisole. In order to control the polymerization process, the corresponding initiator, ethyl 2-bromoisobutyrate, was also added for bulk polymerization. The mixture was degassed, and argon was bubbled through the mixture for 20 min to ensure that oxygen was removed completely. The mixture was heated at 363 K. After several hours, the polymerization solution was cooled to room temperature to terminate the polymerization. The Si wafer was immersed in THF and rinsed with toluene to remove the adsorbed free poly(methyl methacrylate) (PMMA). The PMMA micropattern was observed by AFM.

Figure 11 shows the AFM image of the line-patterned PMMA ultrathin film. An AFM image revealed that the site-specific polymerization of methacrylate monomer occurred on the micropatterned surface of the ATRP initiator. The height and width of the PMMA layer were *ca.* 6–10 nm and *ca.* 5 μm, respectively. The width estimated from the AFM image is in good agreement of the line width of surface initiator micropatterns. The formation of a PMMA layer was further confirmed by XPS measurement, in which the characteristic peaks attributed to aliphatic carbon, the ether carbon, and carbonyl carbon were observed at 285 eV, 286.5 eV, and 288.8 eV, respectively.

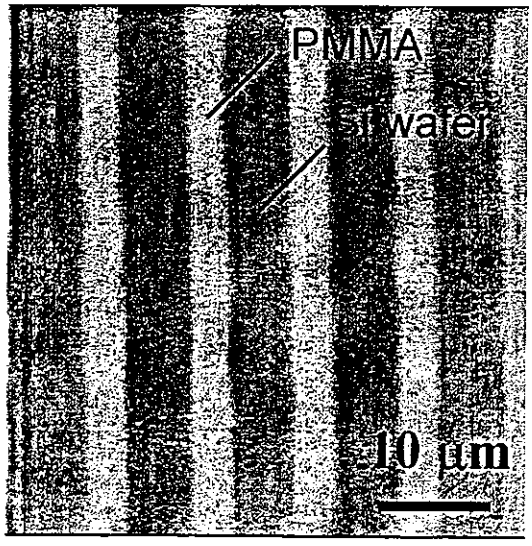

Figure 11. AFM image of line-patterned PMMA ultrathin film.

3.3. Site-specific adsorption of charged microparticles

Two-dimensional alignment of nanoparticles on a substrate surface might be a promising method for fabricating functional materials, since properties of nanoparticles can be tuned by controlling the size and surface chemistry. Various attempts have been made at the site-specific immobilization of micro- and nanoparticles [35, 36]. In this study, the micropatterned organosilane monolayer with an aminosilane/fluoroalkylsilane line pattern was applied for a template surface for site-specific immobilization of negatively charged microparticles.

FHETMS and AEAPDMS were used as surface modifiers for a Si-wafer substrate. The AEAPDMS/FHETMS micropattern (line width, AEAPDMS/FHETMS = 2/4 (μm/μm)) was fabricated by a similar method as that used to yield the multicomponent organosilane monolayer [14, 18, 19, 25]. The Si-wafer substrate with a micropatterned surface was then exposed to the 0.1 g l^{-1} aqueous dispersed solution of sulfonated polystyrene (PS) microparticles (diameter is *ca.* 200 nm, Polyscience) at pH = *ca.* 5.6 for 30 min. The density of the sulfonate group on the microparticle is *ca.* 1 mmol g^{-1}. The substrate was rinsed with distilled water and dried *in vacuo*. We observed the adsorbed PS microparticles on the AEAPDMS/FHETMS monolayer using AFM.

As shown in Fig. 12, the site-specific immobilization of PS particles was successfully achieved on the micropatterned substrate surface. An AFM image shows that the layers consisting of adsorbed PS microparticles are *ca.* 200 nm high and *ca.* 2 μm wide. The height and width estimated from the AFM image are in good agreement with the diameter of PS microparticles and the line width of AEAPDMS

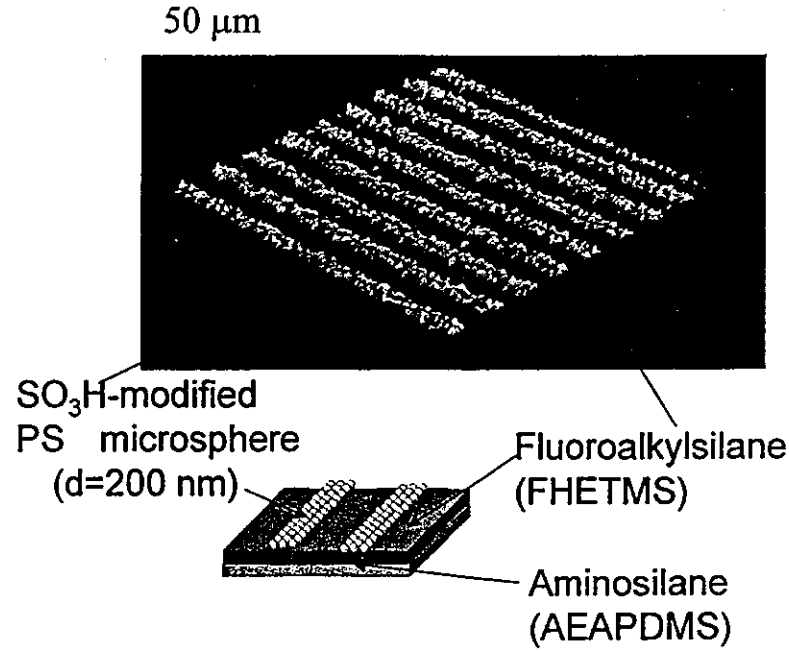

Figure 12. AFM image of the AEAPDMS/FHETMS monolayer after exposure to the aqueous dispersion of sulfonated PS microparticles.

micropatterns, respectively. This result suggests that the sulfonated PS particles were adsorbed on the surface as monolayer. The site-specific adsorption of PS particles onto the AEAPDMS grafted surfaces was ascribed to the electrostatic interaction between negatively charged sulfonic acid groups of PS particles and positively charged amino groups of AEAPDMS-grafted surfaces.

4. CONCLUSIONS

The authors successfully fabricated three-component micropatterned organosilane monolayers on a Si-wafer substrate by a stepwise photolithography process with rotation of a photomask. The line widths of the micropatterned surface corresponded to those of the photomask. Micropatterning of the functional groups influenced the change of surface free energies. Given these results, it should be mentioned that micropatterned organosilane monolayers can be used as model surfaces with controlled, area-selective surface natures, such as free energy, nanostructure, and chemical composition.

Acknowledgements

This research was partially supported by Grant-in-Aid for Scientific Research No. 1200875189, the COE Research 'Design and Control of Advanced Molecular Assembly Systems' (08CE2005) and the 21st Century COE Program, 'Functional Innovation of Molecular Informatics' from the Ministry of Education, Culture, Sports, Science and Technology, JAPAN and also by a grant from the Kawasaki Steel, 21st Century Foundation. We are indebted to Professors Osamu Takai and Hiroyuki Sugimura of Nagoya University for their valuable suggestions made during our research. A. T. also acknowledges Ms. M. Tozu and Dr. T. Hoshi (Ulvac Phi., Co.) for ToF-SIMS measurement.

REFERENCES

1. J. Sagiv, *J. Am. Chem. Soc.* **102**, 92 (1980).
2. K. Kojio, A. Takahara and T. Kajiyama, *Langmuir* **16**, 9314 (2000).
3. S.-R. Ge, K. Kojio, A. Takahara and T. Kajiyama, *J. Biomater. Sci. Polymer Edn* **9**, 131 (1998).
4. A. Takahara, Y. Hara, K. Kojioand and T. Kajiyama, *Coll. Surf. B* **23**, 141 (2002).
5. J. Gun and J. Sagiv, *J. Colloid Interface Sci.* **112**, 457 (1986).
6. J. Gun, R. Iscovici and J. Sagiv, *J. Colloid Interface Sci.* **101**, 201 (1984).
7. E. Lindner and E. Arias, *Langmuir* **8**, 1195 (1992).
8. T. Sato, D. G. Hasko and H. Ahmed, *J. Vac. Sci. Tech. B* **15**, 45 (1997).
9. M. Matsuzawa, S. Tokumitsu, W. Knoll and H. Sasabe, *Langmuir* **14**, 5133 (1998).
10. R. Maoz, E. Frydman, S. R. Cohen and J. Sagiv, *Adv. Mater.* **12**, 725 (2000).
11. A. Hozumi, H. Sugimura, K. Hiraku, T. Kameyama and O. Takai, *Nano Lett.* **1**, 395 (2001).
12. T. Koga, H. Otsuka and A. Takahara, *Trans. Mater. Res. Soc. Jpn.* **27**, 497 (2002).
13. J. M. Calvert and W. J. Dressick, *Jpn. J. Appl. Phys.* **32**, 5829 (1993).

14. H. Sugimura, K. Ushiyama, A. Hozumi and O. Takai, *Langmuir* **16**, 885 (2000).
15. H. Tada and H. Nagayama, *Langmuir* **10**, 1472 (1994).
16. H. Tada, K. Shimoda and K. Goto, *J. Electrochem. Soc.* **142**, L230 (1995).
17. P. W. Hoffmann, M. Stelzle and J. F. Rabolt, *Langmuir* **13**, 1877 (1997).
18. A. Hozumi, K. Ushiyama, H. Sugimura and O. Takai, *Langmuir* **15**, 7600 (1999).
19. T. Koga, H. Otsuka and A. Takahara, *Chem. Lett.*, 1196 (2002).
20. W. Kern, *J. Electrochem. Soc.* **137**, 1887 (1990).
21. S.-R. Ge, A. Takahara and T. Kajiyama, *J. Vac. Sci. Tech. A* **12**, 2530 (1994).
22. K. M. R. Kallury and M. Thompson, *Langmuir* **8**, 947 (1992).
23. A. Takahara, K. Kojio and T. Kajiyama, *Ultramicroscopy* **91**, 203 (2002).
24. D. K. Owens and R. C. Wendt, *J. Appl. Polym. Sci.* **13**, 1741 (1969).
25. A. Kumar, H. A. Biebuyk and G. M. Whitesides, *Langmuir* **10**, 1498 (1994).
26. N. L. Abott, J. P. Folkers and G. M. Whitesides, *Science* **257**, 1380 (1992).
27. J. M. Calvert, *J. Vac. Sci. Tech.* **B11**, 2155 (1993).
28. H. Gau, S. Herminghaous, P. Lenz and R. Lipowsky, *Science* **283**, 46 (1999).
29. C. R. Kagan, T. L. Breen and L. L. Kosbar, *Appl. Phys. Lett.* **79**, 3536 (2001).
30. P. Calvert, *Chem. Mater.* **13**, 3299 (2001).
31. J. S. Wang and K. Matyjaszewski, *J. Am. Chem. Soc.* **117**, 5614 (1995).
32. K. Matyjaszewski and J. Xia, *Chem. Rev.* **101**, 2921 (2001).
33. M. Ejaz, K. Ohno, Y. Tsujii and T. Fukuda, *Macromolecules* **33**, 2870 (2000).
34. X. Kong, T. Kawai, J. Abe and T. Iyoda, *Macromolecules* **34**, 1837 (2001).
35. Y. Masuda, M. Itoh, T. Yonezawa and K. Koumoto, *Langmuir* **18**, 4155 (2002).
36. H. Fudouzi, M. Kobayashi and N. Shinya, *Langmuir* **18**, 7648 (2002).

Transactions of the Materials Research Society of Japan Vol.28 85-88 (2003)

Analysis of Aggregation States of Polymer Thin Films Based on Grazing Incidence X-ray Diffraction

Tomoyuki Koga[1], Masamichi Morita[1,2], Hideomi Ishida[1], Hirohiko Yakabe[1], Sono Sasaki[1]
Osami Sakata[3] and Atsushi Takahara[1,4]*
[1]Graduate School of Engineering, Kyushu University, Hakozaki, Higashi-ku, Fukuoka 812-8581, JAPAN
[2]Fundamental Research Department, Chemical Division, Daikin Industries, Ltd.,
Hitotsuya, Settsu-shi, Osaka 566-8585, JAPAN
[3]Experimental Facilities Division, Japan Synchrotron Radiation Research Institute/SPring-8,
Mikazuki, Sayo, Hyogo 679-5198, JAPAN
[4]Institute for Materials Chemistry and Engineering, Kyushu University, Hakozaki, Higashi-ku,
Fukuoka 812-8581, JAPAN,
Tel: 81-92-642-2721, Fax: 81-92-642-2715, e-mail: takahara@cstf.kyushu-u.ac.jp

Grazing-incidence X-ray diffraction (GIXD) of organosilane monolayers and poly(3-hexylthiophene) was carried out. The in-plane structure of organosilane monolayers depended on the alkyl chain length and preparation method. With an increase in alkyl chain length($CH_3(CH_2)_{n-1}$) from n=18 to 20, the monolayers changed from the hexagonal phase to the rectangular phase. Also, it was revealed that the organosilane monolayers prepared by water-cast method formed order structure compared with those prepared by chemisorption. Poly(3-hexylthiophene) films were prepared onto various substrates and the degree of orientation of side-chain lamellae was studied by GIXD and conventional symmetrical reflection methods. The symmetrical reflection method suggested that the side-chain lamellae were highly oriented perpendicular to the surface of the films. On the other hand, GIXD implied that the lamellar orientation near the surface was disordered in comparison with the bulk.
Key words: Grazing incidence X-ray diffraction, organosilane monolayer, poly(3-hexylthiophene), in-plane structure

1. INTRODUCTION

The aggregation structure of organic ultrathin films has received much attention because of their applications to electronic devices and surface functional nano-coatings. Since X-ray diffraction of an organic ultrathin film obtained by conventional and laboratory-scale X-ray source was weak in intensity, little investigation has been done on their structural analyses. Grazing incidence X-ray diffraction (GIXD) using evanescent X-rays has been applied for the analysis of in-plane molecular aggregation structure of organic ultrathin films.[1,2] In order to carry out precise structural analyses, it is necessary to utilize a highly monochromatic beam from the synchrotron radiation source as the incident X-rays. In this study, the molecular aggregation structures of poly(alkylthiophene) and organosilane monolayers were investigated by GIXD.

2. EXPERIMENTAL

2.1 Sample Preparation

Figure 1 shows the chemical structure of organosilanes and poly(3-hexyl thiophene). The octadecyltrichlorosilane (OTS, Chisso Co., Ltd.), eicosyltrichlorosilane (EITS, Shin-Etsu Chemical Co., Ltd.), docosyltrichlorosilane (DOTS, Shin-Etsu Chemical Co., Ltd.), octadecyltrimethoxysilane (OTMS, Gelest Co., Ltd.), perfluorohexylethyltrimethoxysilane (FHETMS, Fluorochem Co., Ltd.), perfluoropolyethertrimethoxysilane (PFPE, Mw=4,000, Daikin Industries Ltd.) were used for preparation of monolayer.

Figure 2 shows the schematic representation of preparation processes of organosilane monolayers. OTS,

$CH_3(CH_2)_{17}SiCl_3$
octadecyltrichlorosilane (OTS : C18)
$CH_3(CH_2)_{19}SiCl_3$
eicosyltrichlorosilane (EITS : C20)
$CH_3(CH_2)_{21}SiCl_3$
docosyltrichlorosilane (DOTS : C22)
$CH_3(CH_2)_{17}Si(OCH_3)_3$
octadecyltrimethoxysilane (OTMS)
$CF_3(CF_2)_5CH_2CH_2Si(OCH_3)_3$
perfluorohexylethyltrimethoxysilane (FHETMS)
$C_3F_7(OCF_2CF_2CF_2)nOCF_2CF_2CH_2CH_2Si(OCH_3)_3$
perfluoropolyethertrimethoxysilane (PFPE, Mw=4000)

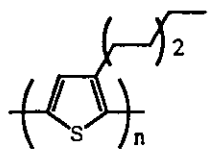

Figure 1 Chemical structures of organosilane compounds and poly(3-hexylthiophene).

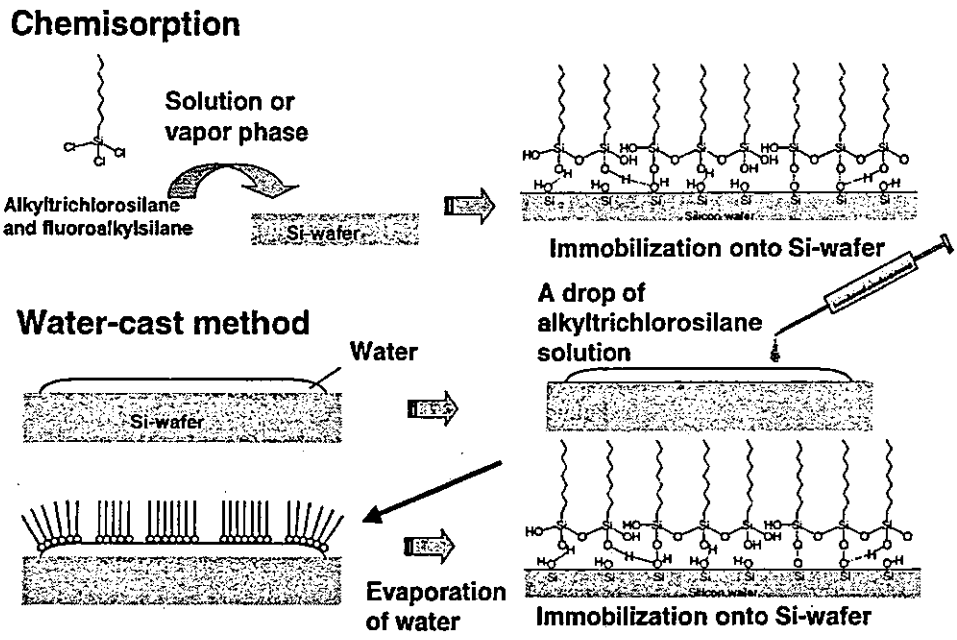

Figure 2 Schematic representation of the preparation of organosilane monolayers.

EITS, DOTS, OTMS, FHETMS were purified by vacuum distillation. PFPE was used without purification. Toluene was refluxed with calcium hydrate for 2h and distilled because organotrichlorosilane is sensitive to moisture. Bicyclohexyl was dried with molecular sieves. The substrates used in this study were Si-wafers cleaned by piranha solution and irradiation of vacuum ultraviolet ray (λ=172 nm) for 10 min under 15 mmHg.[3,4] OTS, EITS, and DOTS monolayers were prepared onto a substrates from their bicyclohexyl (Tokyo Kasei, Co., Ltd.) 5mM solutions by the chemisorption method under N_2 atmosphere at room temperature.[5] Samples were rinsed by successive bicyclohexyl, toluene and ethanol. A PFPE monolayer was prepared by the chemisorption method from its 0.2 % perfluorohexane (3M Co., Ltd.) solution in the same way. Perfluorohexane was used without further purification.

In order to prepare highly ordered monolayers, OTS, EITS and DOTS monolayers were prepared onto substrates by a water-cast method from their 5 mM toluene solutions.[6] Nano-pure water droplets with the total volume of ca. 0.8 mL were spread onto a cleaned Si-wafers with area of ca. 5 cm^2. The toluene solution with a volume of 5 μL was subsequently spread in order to cover completely the water surface with organosilane molecules. The organosilane monolayers were finally obtained after water evaporation at room temperature. OTMS and FHETMS monolayers were prepared by the chemical vapor adsorption method.[4,7,8] The substrates were placed together with a glass tube filled with 0.2 mL organosilane liquid into 65 mL Teflon™ container. The container was sealed with a cup and stainless container. Then the container was placed in an oven maintained at 423 K (OTMS monolayer) and 373 K (FHETMS monolayer) for 2 h. The samples were rinsed with ethanol and dried in vacuo.

In order to investigate the effects of surface free energy of substrates on chain-packing structure of polymer thin films, poly(3-hexylthiophene) (P3HT, Sigma-Aldrich Co., Ltd.) with head-to-head regioregularity of 98.5% and Mw=87k was spin-coated on Si substrates treated with various organosilanes. P3HT thin films with a thickness of ca.100nm were prepared onto the substrate by spin-coating from their chloroform solution. The sample was annealed at 473K for 30min.

2.2 Symmetrical Reflection Method

X-ray diffraction measurements were carried out by using a Rigaku RINT2500 with CuK_α X-ray source in the symmetrical reflection geometry.

2.3 GIXD

The GIXD measurements were carried out at a BL13XU beam line of SPring-8 using incident X-rays with the wavelength, λ of 0.123 or 0.128 nm. In GIXD measurements, strong diffraction was observed for ultrathin films when the incident angle (α_i) to the sample was below a critical angle (α_c).[5] In this condition, X-rays undergo the total external reflection and penetrate into the sample as evanescent waves. The α_c of organosilane was ca. 0.15°. Therefore, in order to analyze the near-surface structure of organic ultrathin films, GIXD measurements were carried out at α_i=0.10°. Diffraction from the sample was detected in the in-plane direction by a scintillation counter. Moreover, a sample cell with polyimide windows was attached to a sample stage. Helium gas was passed through the cell during the GIXD measurement to prevent the sample from its oxidation. The background-corrected GIXD profiles were analyzed by using a curve-fitting method with the Lorentzian function. All measurements were carried out at room temperature.

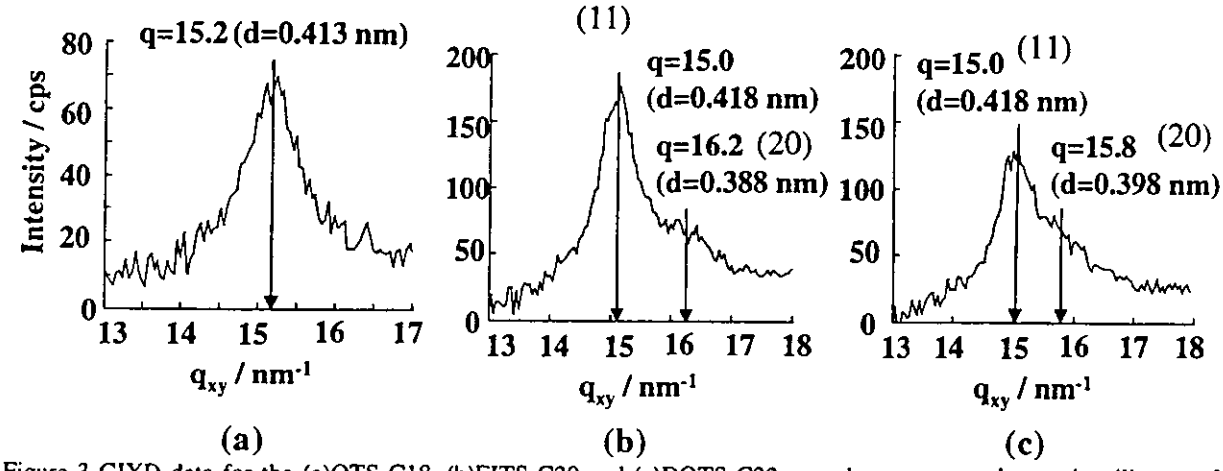

Figure 3 GIXD data for the (a)OTS-C18, (b)EITS-C20 and (c)DOTS-C22 monolayers prepared onto the silicon wafer substrate by water-cast method.

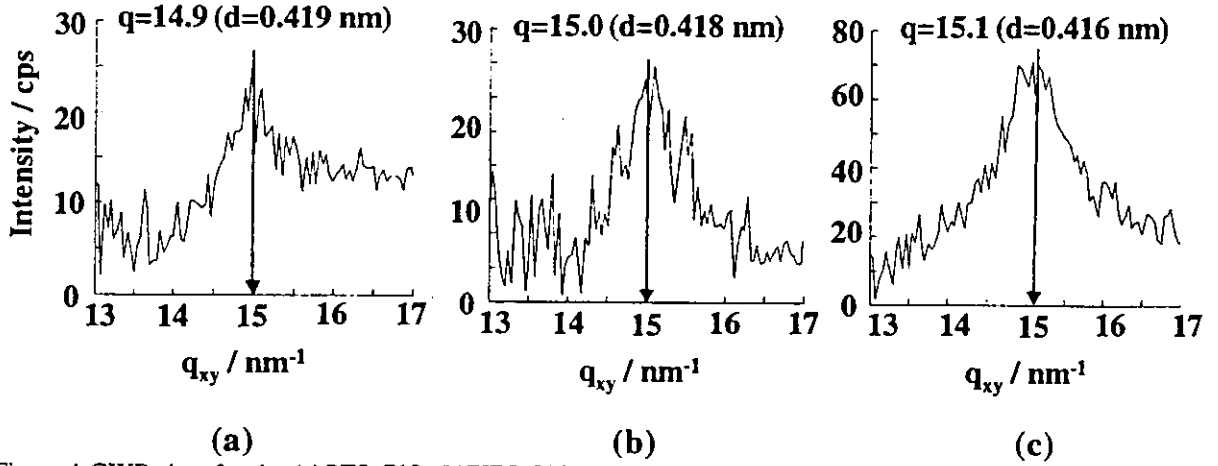

Figure 4 GIXD data for the (a)OTS-C18, (b)EITS-C20 and (c)DOTS-C22 monolayers prepared onto the silicon wafer substrate by chemisorption method.

3.RESULTS AND DISCUSSION

3.1 Oraganosilane Monolayers

Figure 3 shows GIXD profiles for the OTS-C18(a), EITS-C20(b), and DOTS-C22(c) monolayers prepared onto Si-wafer substrates by the water-cast method. In our previous report, ED and GIXD measurements revealed that the (10) spacing of the hexagonal lattice of the OTS-C18 monolayer was ca. 0.42 nm.[5,9,10] Taking into account the result obtained by the ED measurements, it can be considered that the peaks observed in Figure 3(a) is assigned to the (10) reflection of the hexagonal crystal of the OTS-C18 monolayer. The peak of the hexagonal (10) reflection was observed at $q_{xy,max}$ = 15.1 ~ 15.3 nm^{-1}.

On the other hand, in Figure 3(b) and 3(c), a main peak and a shoulder were observed at $q_{xy,max}$ = 15.8 ~ 16.3 nm^{-1} and 15.0 nm^{-1}, respectively. Calculated (20) and (11) spacing of EITS-C20 and DOTS-C22 monolayer were ~0.42 nm and ~0.40nm. In our previous report, the authors revealed that the (20) and (11) spacings of the rectangular lattice of the OTS-C18 monolayer at 223 K were ca. 0.42 and 0.40 nm by the ED measurements, respectively.[10] Therefore, it is most likely that the peaks observed in Figure 3(b) and 3(c) can be assigned to the (20) and (11) reflection of the rectangular crystal of the EITS-C20 and DOTS-C22 monolayers. Thus, these results apparently indicate that the EITS-C20 and DOTS-C22 molecules in the monolayer state are more tightly packed one another at room temperature in comparison with the OTS-C18 molecules in that state.

Figure 4 shows GIXD data for the OTS-C18(a), EITS-C20(b), and DOTS-C22(c) monolayers prepared onto Si-wafer substrates by the chemisorption method. In Figure 4, peaks assigned to the (10) reflection of the hexagonal crystal were observed at $q_{xy,max}$ = 14.9 ~ 15.0 nm^{-1}. The $q_{xy,max}$ slightly shifted to the larger q range with increasing the length of alkyl chain. In our previous study, lateral force microscopy, Fourier transform-infrared spectroscopy, and ED revealed that the packing density of alkylsilane molecules in the monolayers depends on their chain length.[10] Thus, it seems reasonable to consider that decrease of the hexagonal (10) spacing of alkylsilane monolayer is due to the increase of *van der Waals* interaction among their long alkyl chains. However, no crystalline diffraction peaks was observed for the OTMS monolayer prepared by the chemical vapor adsorption method. Since deposition was made above the melting temperature of OTMS, the alkyl chain was immobilized on the Si-substrate in the disordered state.

3.2 P3HT thin films

Poly(alkylthiophene) is one of candidates of polymer

FET devices. The molecular alignment of the conducting polymer thin film might influence the charge carrier transport properties.[11] In order to investigate effects of surface free energy of substrates on chain-packing structure of polymer thin films, P3HT was spin-coated on Si substrates treated with various organosilanes. Figure 5 shows XRD ($2\theta/\theta$ symmetrical reflection method) (a) and in-plane GIXD profiles (b) of P3HT spin-coated films prepared on surface-treated Si-wafers. Each film was annealed at 473 K for 30 min. Rf, PFPE, and Rh indicate the Si-wafers whose surface was treated with FHETMS monolayer, PFPE film, and OTMS monolayer, respectively. SiOH indicates the native oxide Si-wafer. Annealing effect was observed as a sharpening of the diffraction peaks, an appearance of higher-order peaks and decrease in intensity of the amorphous scattering. In the case of symmetrical reflection method the strong (100) reflection (d = 1.60 nm) corresponding to the side-chain lamellar stacking distance is observed. Even though the surface free energy of the substrate changed from ca.12 to 73 mN m^{-1}, a difference was hardly observed among their XRD profiles. On the other hand, in-plane GIXD profiles exhibited the (010) reflection (d = 0.38 nm) corresponding to the π-π stacking of the thiophene ring as well as the (100) reflection. These GIXD profiles also implied that chain-packing structure of P3HT might be independent of the magnitude of surface free energy of the substrates. On the other hand, the comparison between symmetrical reflection and GIXD revealed that the orientation of side-chain lamellar is distorted at the near surface region.

4. CONCLUSION

GIXD was applied for the structural analysis of organosilane monaolayers and polyalkylthiophene thin films. It was revealed that the molecular-packing structure of alkyltrichlorosilane monolayers was strongly depended on the preparation method and alkyl chain length. GIXD was also applied for the surface structural analysis of P3HT thin films. It was revealed that there was no appreciable influence of substrate on the side chain orientation in the near-surface region.

Acknowledgement

The synchrotron radiation experiments were performed at SPring-8 with the approval of JASRI as Nanotechnology Support Project of The Ministry of Education, Culture, Sports, Science and Technology, 2002B5115-NS2-np and 2003A0606-ND1-np.

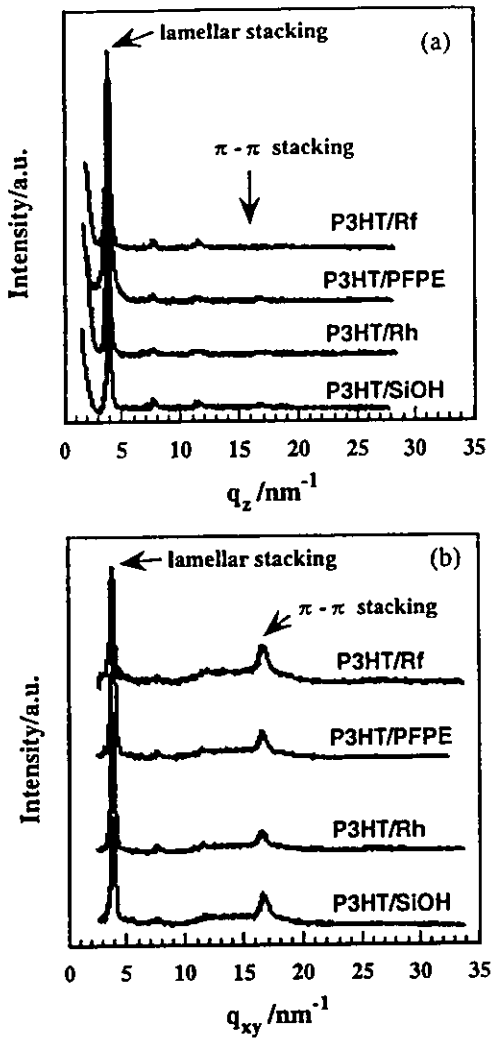

Figure 5 (a) XRD(symmetrical reflection method) and (b) GIXD profiles of P3HT spin-coated films on Si-wafer with different surface treatment.

References

[1] R. Maoz, J. Sagiv, D. Degenhardt, H. Mohwald and P. Quint, *Supramol. Sci..*, **2**, 9(1995).

[2] V. M. Kaganer, G. Brezesinski, H. Mohwald, P. B. Howes and K. Kjaer, *Phys. Rev. E*, **59**, 2141(1999).

[3] T. Kajiyama, S. -R. Ge, K. Kojio and A. Takahara, *Supramol. Sci.*, **3**, 123(1996).

[4] H. Sugimura, K. Ushiyama, A. Hozumi and O. Takai, *Langmuir*, **16**, 885(2000).

[5] K. Kojio, K. Omote, A. Takahara and T. Kajiyama, *Langmuir*, **16**, 3932(2000).

[6] K. Kojio, K. Tanaka, A. Takahara and T. Kajiyama, *Bull. Chem. Soc., Japan*, **74**, 1397 (2001).

[7] H. Tada and H. Nagayama, *Langmuir*, **10**, 1472(1994).

[8] T. Koga, H. Otsuka and A. Takahara, *Chem. Lett*, 1196(2002).

[9] K. Kojio, S.-R. Ge, A. Takahara and T. Kajiyama, *Langmuir*, **14**, 971(1998).

[10] K. Kojio, A. Takahara and T. Kajiyama, *Langmuir*, **16**, 9314(2000).

[11] T A. Chen, X. M. Wu and R. D. Ricke, *J. Am. Chem. Soc.*, **117**, 233(1995).

(Received July 21, 2003; Accepted August 21, 2003)

Transactions of the Materials Research Society of Japan 29[6] 2873-2876 (2004)

Physicochemical Properties and Bio-degradation of Segmented Polyurethane and Poly(urethane-urea) Derived from Lysine-Based Diisocyanate

Tomohiro Yamaguchi[1], Hideyuki Otsuka[1,2], Satoru Kidoaki[3], Takehisa Matsuda[3], Atsushi Takahara[1,2]*

[1]Graduate School of Engineering, Kyushu University, Hakozaki, Higashi-ku, Fukuoka 812-8581, JAPAN
[2]Institute for Materials Chemistry and Engineering, Kyushu University, Hakozaki, Higashi-ku, Fukuoka 812-8581, JAPAN
[3]Biomedical Engineering, Graduate School of Medicine, Kyushu University, Maidashi, Higashi-ku, Fukuoka 812-8582, JAPAN
Tel: 81-92-642-2721, Fax: 81-92-642-2715, e-mail: takahara@cstf.kyushu-u.ac.jp

Segmented polyurethanes (SPU) and poly(urethane-urea)s (SPUU) which were expected to yield non-toxic degradation products were synthesized from lysine-based diisocyanate (LDI), 1,3-propanediol (PDO), 1,4-butanediamine (BDA), and polycaprolactone diol (PCL). SPU and SPUU were synthesized via a standard two-step prepolymer method. The hard segment fraction was changed in order to tune the mechanical properties and the degradability. The aggregation structures of the SPU and SPUU were characterized by IR spectroscopy and DSC. IR spectroscopy revealed that fraction of hydrogen bonded urethane and urea carbonyl groups increases with an increase in hard segment fraction. DSC thermogram revealed that the glass transition temperature of BDA-based hard segment is higher than that of PDO-based one. Tensile tests revealed the excellent elastic properties of PCL(1250)(71)BDA. Furthermore, the degradation of SPU and SPUU were investigated by exposing the polymers to buffer solution at 310 K (pH=7.6). The degradation rate of SPU increased with an increase in soft segment fraction. This is because the soft segment has the hydrolyzable ester linkages and is susceptible to hydrolysis compared with that of the urethane linkage. Finally, an electrospray deposition method was used to fabricate biodegradable SPU micro-fibers. FE-SEM images showed that higher concentration of solution favored to form of uniform biodegradable micro-fibers without beads-like structure.

Key words: Degradation, Lysine-based diisocyanate, Polyurethanes, Poly(urethane-urea)s, Electrospray Deposition

1. INTRODUCTION

The use of degradable polymers in tissue engineering for replacement or repair of wide range of tissues is an area of intensive research in recent years. A variety of biodegradable polymers have been developed in the last two decades. However, the majority of these polymers are typically hard and brittle plastic and few biodegradable elastomeric polymers have been synthesized.[1]

The recent development of diisocyanates based on lysine has removed an obstacle to synthesizing biodegradable elastomers expected to yield non-toxic degradation products.[2] It was surmised that if the diisocyanate were liberated by hydrolysis of the urethane bonds of the polymer during degradation the isocyanate functionalities would react with water to regenerate the lysine derivative, an essentially non-toxic products.

Recently, there has been growing interest in a fiber production technology known as electrospray deposition (ES). ES is unique as a fiber spinning process because it can change the morphology and diameter depending on the processing parameter such as solution concentration and applied electric field strength.[3] ES can produce highly porous non-woven fabrics consisting of well-defined fibers which are used for tissue engineering.

In this study, the segmented polyurethanes (SPU) and segmented poly(urethane-urea)s (SPUU) were synthesized from lysine-based diisosyanate. The physical and structural characterizations of SPU and SPUU were performed using differential scanning calorimetry and IR spectroscopy. Then the mechanical properties were investigated by stress-strain measurement. The degradation behavior of SPU and SPUU were also investigated. ES technique was used to fabricate biodegradable fibers. The morphology of electrospray deposited fiber was investigated by field-

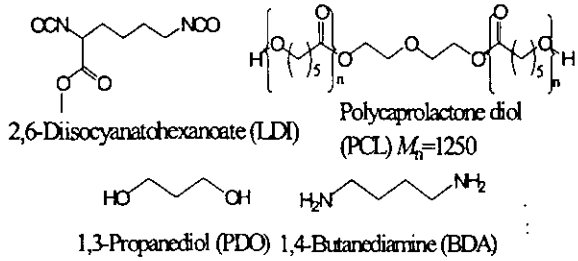

Figure 1 Chemical structures of diisosyanate, soft segment polyol, and chain extenders.

Table 1 Ratio of LDI, PCL, and chain extenders and soft segment concentration of SPU and SPUU.

Sample	LDI: PCL: Chain Extender	Chain Extender	Soft Segment Fraction (wt%)
PCL(1250)(100)PDO	4:4:0	PDO	100
PCL(1250)(80)PDO	4:2:2	PDO	80
PCL(1250)(69)PDO	4:1.5:2.5	PDO	69
PCL(1250)(56)PDO	4:1:3	PDO	56
PCL(1250)(0)PDO	4:0:4	PDO	0
PCL(1250)(80)BDA	4:3:1	BDA	80
PCL(1250)(75)BDA	4:2.5:1.5	BDA	75
PCL(1250)(71)BDA	4:2:2	BDA	71
PCL(1250)(64)BDA	4:1.5:2.5	BDA	64
PCL(1250)(53)BDA	4:1:3	BDA	53
PCL(1250)(0)BDA	4:0:4	BDA	0

emission scanning electron microscopy (FE-SEM).

2. EXPERIMENTAL

2.1 Materials

Fig. 1 shows the chemical structures of 2,6-diisocyanatohexanoate (LDI), polycaprolactone diol (PCL), 1,3-propandiol (PDO), and 1,4-butanediamine (BDA). 2,6-Diisocyanatohexanoate (LDI, Kyowa Hakko Co., Ltd.), polycaprolactone diol (PCL, Aldrich Chemical), 1,3-propandiol (PDO, Kanto Chemical. Co., Ltd.), and 1,4-butanediamine (BDA, Aldrich Chemical) were used for the preparation of SPU and SPUU.

LDI, PDO, and BDA were purified by vacuum distillation. PCL was placed in a vacuum oven at 353 K for 24 h to remove residual water before reaction. Dimethylformamide (DMF, Nacalai Tesque, Co., Ltd) was purified by vacuum distillation. Di-*n*-butyltin dilaurate (Tokyo Kasei Kogyo Co., Ltd.) was used as a catalyst for the synthesis of SPU.

2.2 Synthesis of SPU and SPUU

SPU and SPUU were synthesized via a standard two-step prepolymer method and the ratio of soft segment to chain extender was changed.[4] Excess LDI was reacted with PCL. The prepolymer reaction proceeded for 150 min at 358 K. Then the chain extenders (PDO for SPU and BDA for SPUU) was added to the prepolymer and allowed to react for 48 h (SPU) in the presence of 0.1 % of catalyst and for 1 h (SPUU) in DMF. The polymer was then immersed in distilled water for 48 h and dried under vacuum at 353 K for 24 h to remove water.[5] The composition of SPU and SPUU was given in Table 1. Sample names were designated as soft segment (soft segment M_n) (soft segment fraction) chain extender.

All solid films were prepared by solution casting. The SPU and SPUU were dissolved in THF (SPU) and DMF (SPUU). The cast films were dried under vacuum at 393 K for 24 h.

2.3 Characterization of SPU and SPUU

Fourier transform infrared (FT-IR) spectra were obtained with a Spectrum One (Perkin-Elmer. Co., Ltd.) infrared spectrometer. Spectra were generated from 64 scans at 0.5 cm^{-1} resolution. 5 % THF solution of SPU was placed directly onto NaCl and 5 % DMF solution of SPUU were placed directly onto CaF_2. Subsequent evaporation of the DMF at 393 K under vacuum was performed for 24 h.

DSC thermograms from 173 K to 423 K were obtained using a differential scanning calorimeter DSC8230B (Rigaku Denki Co. Ltd.) at a heating rate of 15 K min^{-1} under a dried nitrogen purge. The sample weight was around 8 mg.

Stress-strain measurements were obtained at room temperature using an RTC-1250 (ORIRNTEC. Co., Ltd.). Samples were cut from films cast to 90-120 μm thickness. A cross-head speed of 200 mm min^{-1} was used.

2.4 SPU and SPUU degradation

Degradation studies were performed using tris-buffered saline (TBS, 0.05 M Tris, 0.1M NaCl, pH=7.6).[5] Each samples were placed into an individual vial containing 10 ml TBS, and incubated at 310 K. Samples were removed from buffer following 7, 21, 35, and 70 days. After drying under vacuum for 72 h, samples were reweighed to determine total percentage of mass loss.

2.5 Electrospray Deposition (ES)

For SPU, THF was used as the solvent to prepare the polymer solutions at different concentration for ES. A schematic diagram of the ES device for manufacturing fibers was shown in Fig. 2. The polymer solution was delivered by a programmable pump to the exit hole of the stainless-steel blunt-ended needle electrode (inner diameter; 0.8 mm). An aluminum plate was used as a lower electrode. A positive high DC voltage supply was used to apply the voltage. The flow rate was 1 ml/h. The distance of electrode was 350 mm. The sample solution was electrostatistically drawn from the needle tip and deposited on the lower electrode.

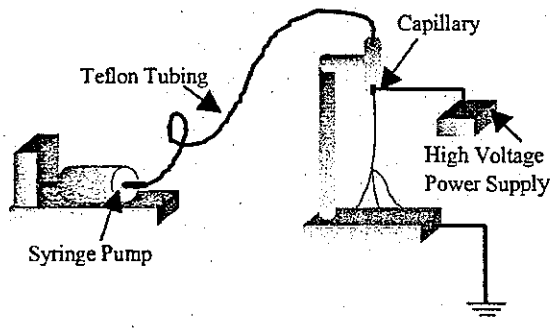

Figure 2 Schematic diagram of the ES apparatus for manufacturing fiber structure.

All the samples were observed with FE-SEM (S-4300SE, Hitachi Co., Ltd.) under the accelerating voltages of 1 kV. The samples were observed without conductive over-coating.

3. RESULTS AND DISCUSSION

3.1 Characterization of SPU and SPUU

Fourier transform infrared (FT-IR) spectroscopy was used to investigate the structural difference in hard and soft segments of SPU and SPUU. IR spectra for the SPU and SPUU are shown in Fig. 3. The absorption bands at 1735 cm^{-1} to 1720 cm^{-1} are associated with the ester carbonyl groups of PCL. The broad shoulders detected at 1670 cm^{-1} to 1710cm^{-1} are assigned to the hydrogen bonded urethane carbonyl group (Fig. 3a). The shoulder from 1620 cm^{-1} to 1680cm^{-1} is ascribed urea carbonyl group (Fig. 3b). The relative intensity of the bands attributed to hydrogen bonded urethane and urea linkage increased with a decrease in hard segment fraction. This result shows that the increase of hydrogen bonding among hard segments with an increase in fraction of chain extender.

The difference in state of molecular aggregation between SPU and SPUU was confirmed by the DSC. The hard segment is amorphous because of the non-symmetric molecular structure of LDI. Fig. 4 shows the DSC thermograms for SPU and SPUU, respectively. A base line shift corresponding to the hard segment glass transition temperature (T_g) was observed in the 308 K in SPU (Fig. 4a). It seems that the non-symmetric diisocyanate (LDI) produces hard segment that was unable to pack efficiently. However, the hard segment T_g was observed 379 K in DSC curves of SPUU. This is because the urea linkage has strong hydrogen bonding compared with that of the urethane linkage. Soft segment crystal melting was observed in the range of 283 K to 320 K (Fig.4a). Crystallinity of SPU decreased

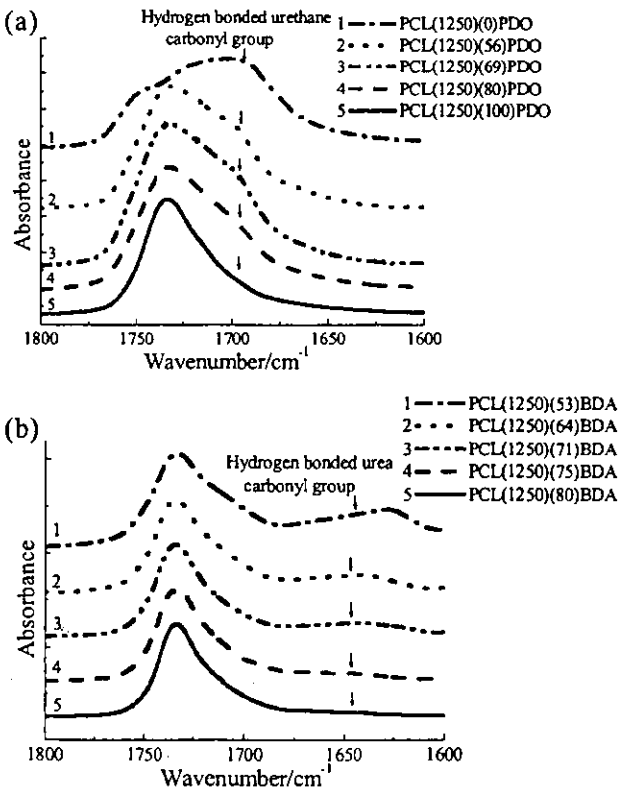

Figure 3 FT-IR absorbance spectra of (a) SPU series and (b) SPUU series.

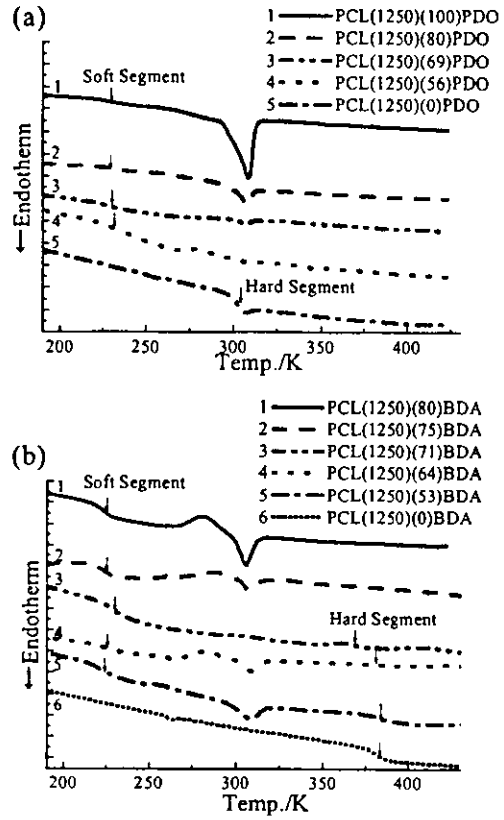

Figure 4 DSC scans of (a) SPU series and (b) SPUU series.

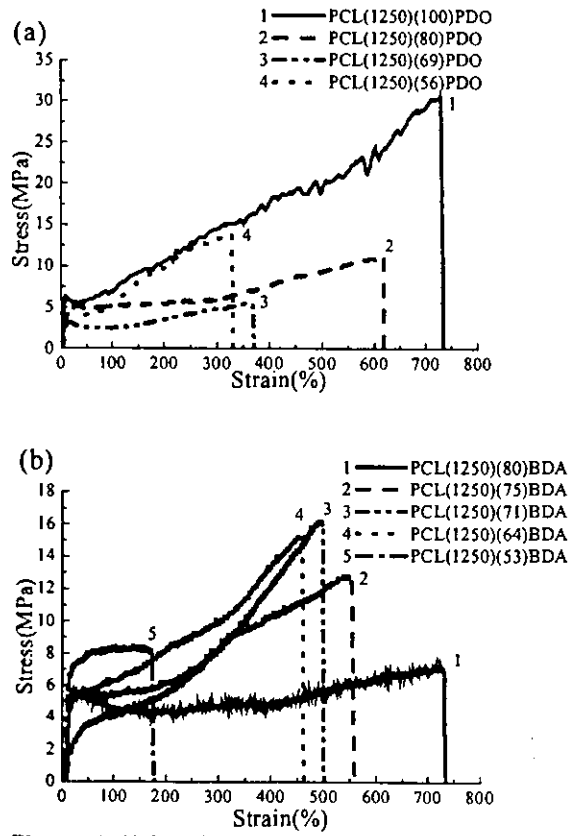

Figure 5 Uniaxial stress-strain curves for (a) SPU series and (b) SPUU series.

with a decrease in PCL fraction. This is due to the partial solubilization of hard segment into PCL phase. PCL(1250)(71)BDA showed higher soft segment T_g than other SPUU's (Fig. 4b). These shifts of T_g are attributed to the partial solubilization of hard segment into PCL phase. Phase separation proceeded with the increase of hard segment because of strong hydrogen bonding.

3.2 Mechanical properties of SPU and SPUU

The mechanical properties of SPU and SPUU were investigated by stress-strain measurement. Typical stress-strain curves for SPU and SPUU are shown in Fig. 5. The results suggested that the increasing modulus and decreasing the ultimate strain with increasing the hard segment fraction of SPU (Fig. 5a). This result showed that the PCL crystallites may act as physical cross-links. In contrast, PCL(1250)(71)BDA showed the excellent elastic properties (Fig. 5b). This is because the BDA formed strong aggregated hard segment and the loss of crystallinity of PCL soft segment.

3.3 Degradation of SPU

The degradation characteristics of a series of SPU were evaluated. The mass loss data for SPU samples were shown in Fig 6. The magnitude of degradation in SPU was increased with an increase in the soft segment fraction. This is because the soft segment has the hydrolyzable ester linkages and is susceptible to hydrolysis compared with that of the urethane linkage.

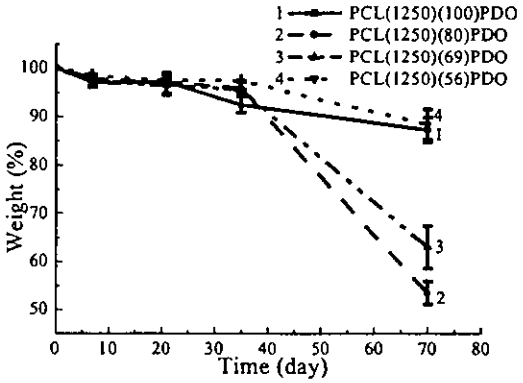

Figure 6 Degradation behavior of SPU in pH=7.6 at 310 K.

3.4 Electrospray deposition (ES)

In ES experiment, morphological change of the deposited ES microstructure is expected when the concentration of polymer solutions were changed. Fig. 7 showed FE-SEM images of SPU. FE-SEM images showed that a mixture of large beads and fibers were formed by ES at 20 wt% PCL(1250)(80)PDO solution under voltage of 13.5 kV (Fig. 7a). In contrast, fine fibers was formed at 30 wt% PCL(1250)(80)PDO solution under voltage of 15.4 kV (Fig. 7b). It was shown that higher concentration of solution favored to form of uniform fibers without beads-like structure. This is because the critical viscosity in solution needs to be exceeded in order to fabricate fibers.[6] Below this viscosity chain entanglement are insufficient to stabilize the jet, leading to spraying of droplets.

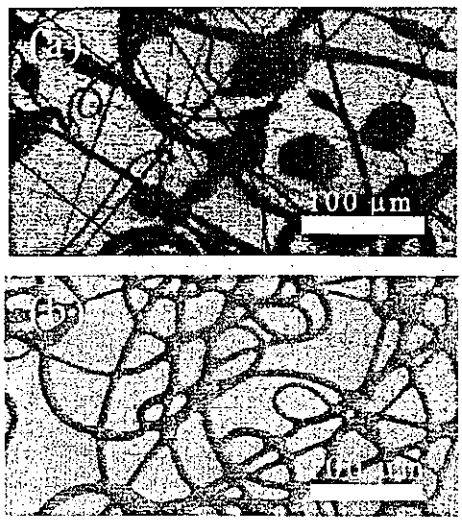

Figure 7 FE-SEM images of microstructure of electrospray deposited PCL(1250)(80)PDO. (a) 20 wt% under voltage of 13.5 kV and (b) 30 wt% under voltage of 15.4 kV.

4. CONCLUSION

Biodegradable segmented polyurethanes (SPU) and segmented poly(urethaneurea)s (SPUU) derived from a lysine-based diisocyanate were synthesized and characterized. IR spectroscopy revealed that the increase of hydrogen bonding among the hard segment with an increase in chain extender fraction. DSC thermogram revealed that the BDA-based hard segment T_g is higher than that of PDO-based one. Tensile tests revealed the excellent elastic properties of PCL(1250)(71)BDA. The magnitude of degradation of SPU was increased with an increase in the soft segment fraction. ES technique was used to fabricate biodegradable fibers. It was shown that higher concentration of solution favored to form of uniform biodegradable micro-fibers without beads-like structure.

Acknowledgement

This work was supported by a Grant-in-Aid for Scientific Research from Ministry of Health, Labor and Welfare (MHLW) of Japan and P&P, Green Chemistry, of Kyushu University.

References

[1] K. A. Athanasiou, G. G. Niederauer and C. M. Agrawal, *Biomaterials.*, **17**, 93(1996).
[2] P. Bruin, G. J. Veenstra, A. J. Nijenhuis, A. J. Pennings, *Makromol Chem Rapid Commun.*, **9**, 589(1988).
[3] J. M. Deitzel, J. Kleinmeyer, D. Harris, N. C. Beck Tan, *Polymer*, **42**, 261(2001).
[4] D. J. Lyman, *J.Polym.Sci.*, **45**, 49(1960).
[5] G. A. Skarja and K. A. Woodhouse, *J. Biomater. Sci. Polymer Edn*, **13**, 391(2002).
[6] E. Kenawy, J. M. Layman, J. R. Watkins, G. L. Bowlin, J. A. Matthews, D. G. Simpson, G. E. Wnek, *Biomaterials*, **24**, 907(2003).

(Received October 11, 2003; Accepted August 31, 2004)

Macromolecular Symposia in press

Charcterization of Novel Bio-degradable Segmented Polyurethanes Prepared from Amino-acid Based Diisocyanate

Atsushi Takahara[1,2]*, *Michiko Hadano*[1], *Tomohiro Yamaguchi*[1], *Hideyuki Otsuka*[1,2], *Satoru Kidoaki*[3], *Takehisa Matsuda*[3]

[1]Graduate School of Engineering, [2]Institute for Materials Chemistry and Engineering, Kyushu University, Hakozaki, Higashi-ku, Fukuoka 812-8581, JAPAN e-mail: takahara@cstf.kyushu-u.ac.jp
[3]Graduate School of Medicine, Kyushu University, Maidashi, Higashi-ku, Fukuoka 812-8582, JAPAN

Summary: Segmented polyurethanes (SPUs) which were expected to yield non-toxic degradation products were synthesized from lysine-based diisocyanate (LDI), 1,3-propanediol (PDO), and polycaprolactone diol (PCL). SPUs were synthesized via a standard two-step prepolymer method. The hard segment fraction was changed in order to tune the mechanical properties and the degradability. The aggregation structures of the SPUs were characterized by infrared spectroscopy and differential scanning calorimetry(DSC), temperature dependence of dynamic viscoelasticity, and small-angle X-ray scattering(SAXS). DSC and dynamic viscoelastic measurements revealed that the glass transition temperature (T_g) of soft segment increased with an increase in hard segment fraction. SAXS of SPUs revealed the aggregation states of hard and soft segments. Furthermore, the degradation of SPUs was investigated by exposing the polymers to buffer solution at 310 K (pH=7.6). The degradation rate of SPUs increased with an increase in soft segment fraction. This is because the soft segment has the hydrolyzable ester linkages and the ester linkages are susceptible to hydrolysis compared with the urethane linkages. Finally, an electrospray deposition method was used to fabricate biodegradable SPU micro-fibers. FE-SEM images showed that higher concentration of solution favored to form uniform biodegradable micro-fibers without beads-like structure.

Keywords: Segmented polyurethane; lysine-based diisocyanate; biodegradation; microfiber, electro-spray deposition

Introduction

A variety of biodegradable polymers have been developed in the last two decades. However, the majority of these polymers are typically hard and brittle plastics and few biodegradable

elastomeric polymers have been synthesized so far [1-3]. The recent development of diisocyanates based on lysine has removed an obstacle to synthesize biodegradable segmented polyurethane (SPU) elastomers expected to yield non-toxic degradation products [4]. If the lysine-based diisocyanate component in SPU was liberated by hydrolysis of the urethane bonds of the polymer during degradation, the product would be a lysine derivative, an essentially non-toxic product.

In this study, the segmented polyeurethanes (SPUs) were synthesized from lysine-based

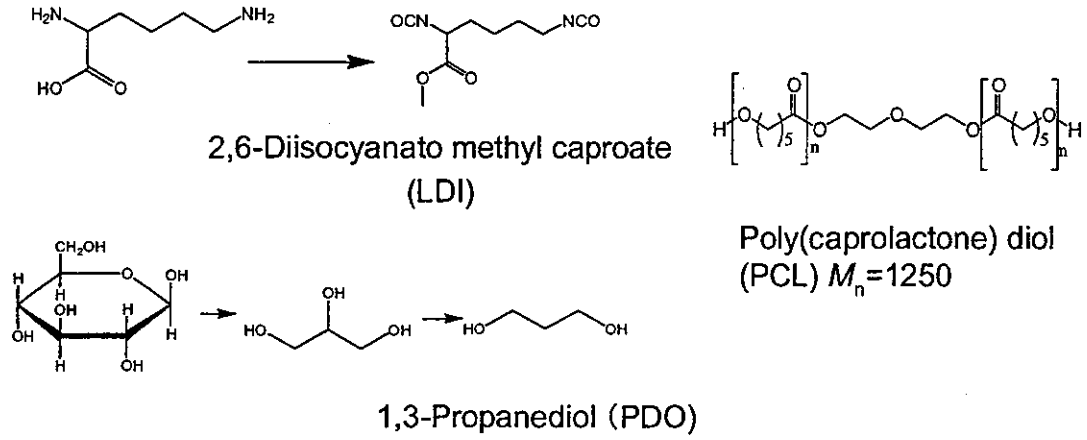

Figure 1 Chemical structures of components of SPU. LDI and PDO can be synthesized from lysine and glucose, respectively.

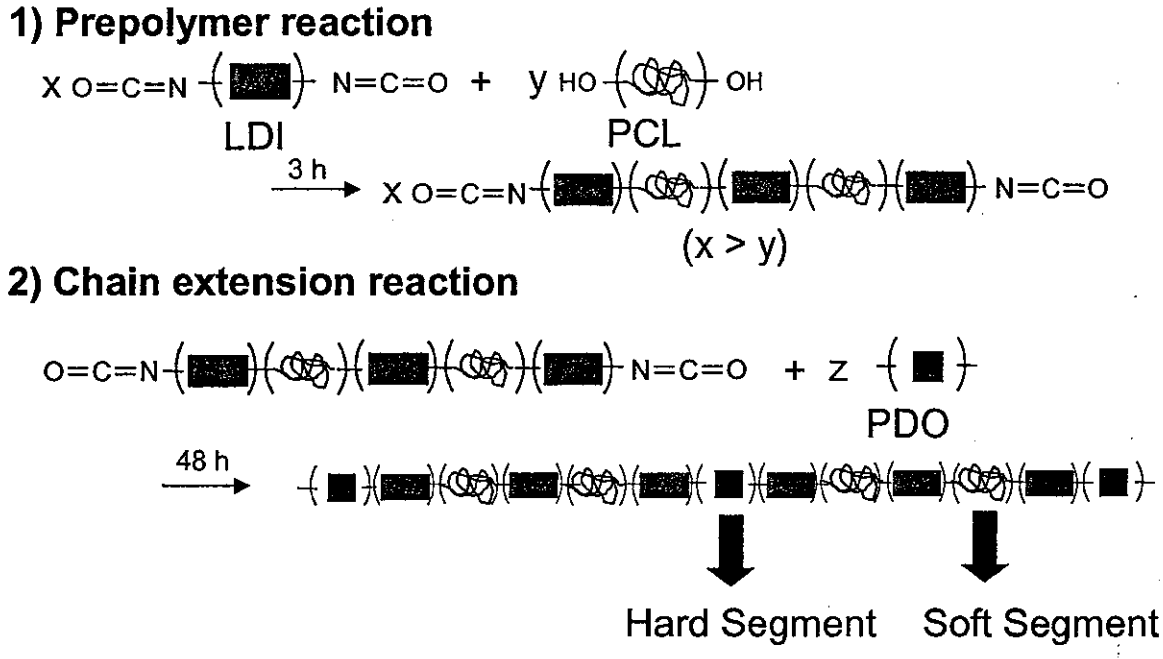

Figure 2 Schematic representation of synthesis of segmented polyurethane(SPU).

diisocyanate. The physical and structural characterizations of SPU were performed. The degradation behavior of SPUs was also investigated. Finally, in order to discuss the possibility of the design of tissue-engineering scaffold, electro-spray deposition (ESD) technique was used to fabricate biodegradable microfibers and microfiber mesh.

Experimental

Materials. 2,6-Diisocyanatohexanoate (LDI), polycaprolactone diol (PCL), and 1,3-propandiol (PDO) were used for the preparation of SPU. PCL with M_n of 1250 was obtained from Aldrich Chemical (Milwaukee, WI, U.S.A.). PCL was placed in a vacuum oven at 333 K to remove residual water before reaction. PDO and LDI were obtained from Kanto Chemical Co. (Tokyo, Japan) and Kyowa Hakko Kogyo Co. (Tokyo, Japan), respectively, and they were distilled under vacuum before use. Their chemical structures were summarized in Figure 1.

Synthesis of Segmented Polyurethanes. SPUs were synthesized via a standard two-step prepolymer method [5,6,7] and the ratio of soft segment to chain extender was changed in order to control the mechanical properties and degradation behavior. Figure 2 shows schematic representation of synthesis of segmented polyurethane(SPU). Excess LDI was reacted with PCL as prepolymer reaction for 150 min at 358 K. Then, the PDO chain extender was added to the prepolymer and allowed to react for 48 h in the presence of dibutyltin dilaurate (0.1 mol%) as a catalyst in *N,N*-dimethylformamide (DMF). The resulted polymer was precipitated by slowly pouring solution into water and the obtained polymer powder was washed with methanol and water. Then, the polymer was dried under vacuum at 353 K for 24 h to remove water. The obtained polymers were multi-block copolymers of hard and soft segments. Soft segment consists of PCL and LDI, whereas hard segment consists of LDI and PDO. Gel permeation chromatography (GPC) was used to determine the molecular weight of SPU. M_w of SPU was in the range of 53k to 86k with M_w/M_n of ca.1.75. Samples were designated as "PCL (M_n of PCL) (PCL fraction) PDO". All solid films were prepared by solution casting from THF solution. The cast films were dried under vacuum at 393 K for 24 h.

Characterization. SPU films were characterized by dynamic viscoelastic measurement, small-angle X-ray scattering (SAXS), Fourier transform infrared (FT-IR) spectroscopy, differential scanning calorimetry (DSC), and tensile tests.

Degradation Behavior. Degradation studies were performed using tris-buffered saline (TBS, 0.05 M Tris, 0.1M NaCl, pH=7.6). Each SPU film with 10 mm x10 mm x 0.9 mm in dimension was placed into an individual vial containing 10 ml TBS, and incubated at 310 K.

Samples were removed from buffer following 7, 21, 35, and 70 days. After drying under vacuum for 72 h, samples were reweighed to determine total percentage of weight loss.

Electro-spray Deposition. Chloroform was used as the solvent to prepare the polymer solutions at different concentration for ESD. The details of ESD equipment was reported elsewhere [8]. The polymer solution was delivered by a programmable pump to the exit hole of the electrode. A positive high-voltage supply was used to supply the voltage. The flow rate was 1 ml h^{-1} and the distance of electrode was 300 mm. The electrosprayed mesh was prepared on to the substrate through continuous deposition with transverse movement of substrate. All the samples were observed with FE-SEM (Hitachi, S-4300) under the accelerating voltages of 1 kV without conductive over-coating.

Results and discussion

Characterization. FT-IR spectroscopy was used to investigate the structural difference in hard and soft segments of SPUs with various PCL fractions. Figure 3 shows the IR spectra of SPUs. The broad shoulders detected at 1730-1750 and 1680-1710cm^{-1} are assigned to the free and hydrogen-bonded urethane and ester carbonyl groups, respectively. The relative intensity of the bands attributed to hydrogen-bonded carbonyl groups increased with an increase in hard segment fraction. This result suggests that hydrogen bonding of carbonyl groups increases with an increase in fraction of PDO chain extender.

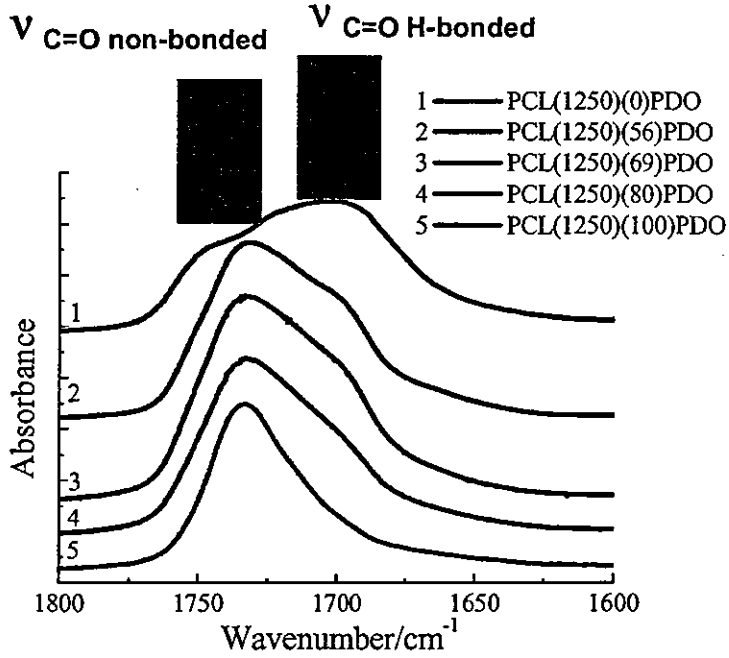

Figure 3 Transmission IR spectra of SPU in the carbonyl stretching region

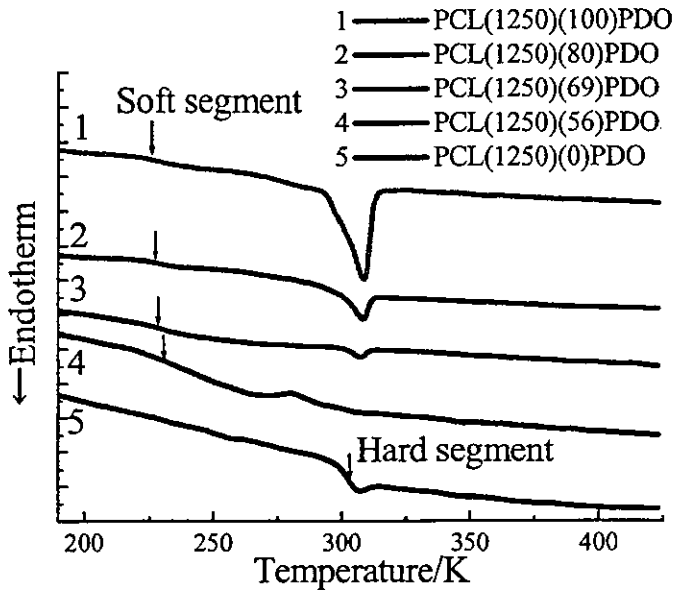

Figure 4 DSC thermograms for SPU with various soft segment contents.

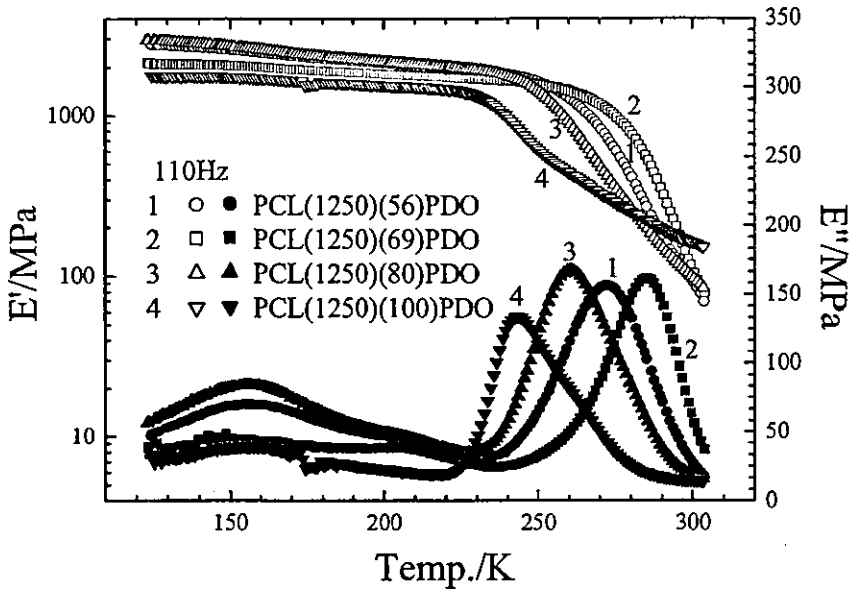

Figure 5 Temperature dependence of dynamic storage modulus, E' and dynamic loss modulus, E" for SPU with various soft segment content.

The difference in state of molecular aggregation of SPUs was confirmed by DSC. Figure 4 shows DSC thermograms for SPU with various soft segment contents. A base line shift corresponding to the hard segment T_g was observed at 302 K. It seems that the non-symmetric diisocyanate (LDI) produces hard segments that were unable to pack efficiently to form crystalline hard segment domain. This also gives the low T_g of hard segment compared with that of aromatic diisocyanate-based hard segment. T_g and crystal melting of PCL in soft segment were observed in the ranges of 225 K to 235 K and 283 K to 320 K, respectively. Crystallinity of PCL in SPUs decreased with a decrease in PCL fraction. This is because of the partial solubilization of hard segment in PCL phase.

The state of thermal molecular motion of SPUs was characterized by dynamic viscoelastic measurement. Temperature dependence of dynamic viscoelasticity was measured at 110Hz from 130 to 310 K under dried nitrogen purge. Figure 5 shows the temperature dependence of dynamic storage modulus, E' and dynamic loss modulus, E" for SPUs with various soft segment contents. A large decrease in E' was observed due to the onset of micro-Brownian motion of PCL soft segment following by the melting of PCL crystallite. Since more than two relaxations were overlapped at around 300 K, it is difficult to separate the relaxation mechanisms at this temperature region. Since the hard segment T_g and melting temperature of PCL were located at ca.300 K, a constant modulus at rubbery plateau was not observed for SPU at above room temperature. Since PCL(1250)(100)PDO does not have low T_g hard segment, a crossover of E' was observed at 280-300K. A broad peak observed at ca.150 K is assignable to γ-absorption of PCL soft segment.

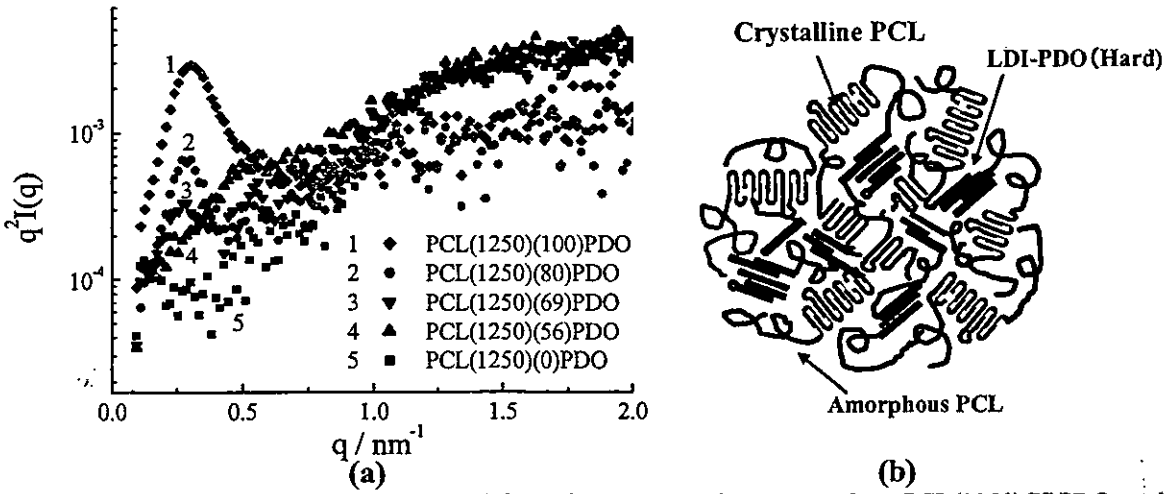

Figure 6 (a) Dependence of corrected intensity on scattering vector for PCL(1250)(X)PDO and (b) structure model of PCL(1250)(X)PDO.

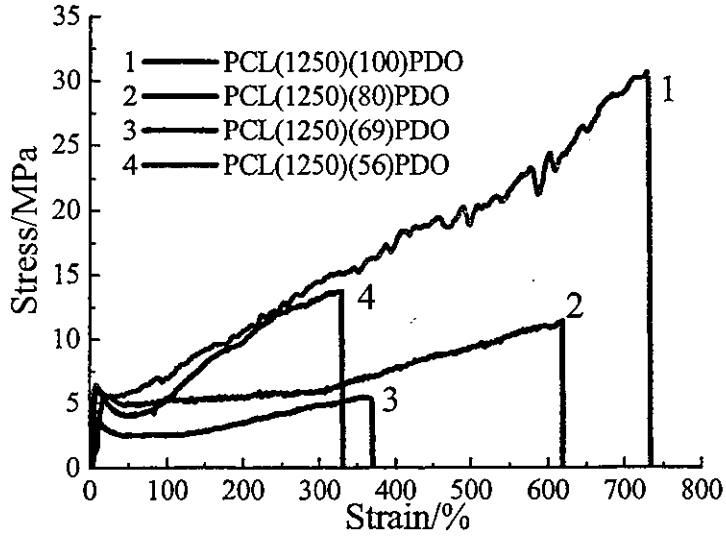

Figure 7 Stress-strain curves for SPU with various soft segment fraction.

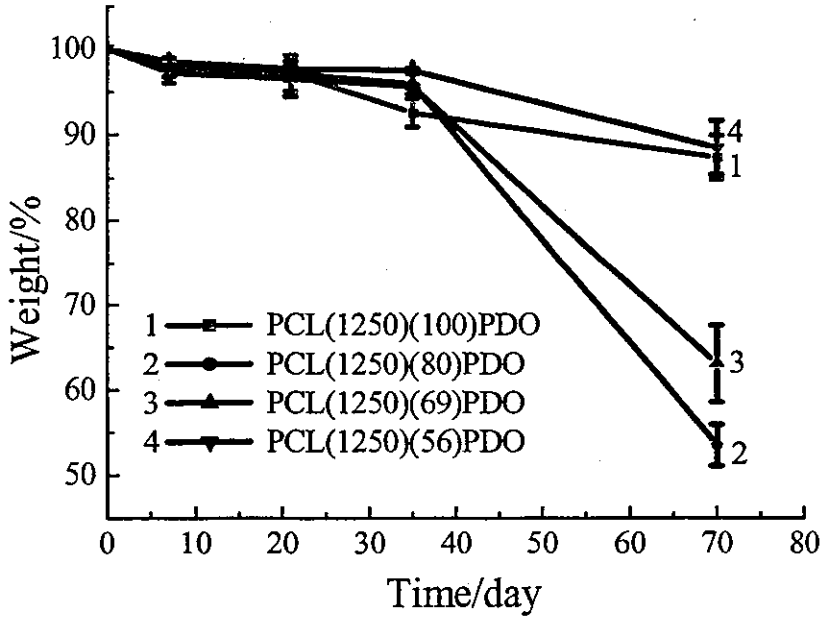

Figure 8 The change in weight with time after immersion in Tris-buffer solution at 310K for SPUs with various soft segment contents.